Mathematical Biosciences 295 (2018) 48–54

Contents lists available at ScienceDirect

Mathematical Biosciences

journal homepage: www.elsevier.com/locate/mbs

Canard phenomenon in a slow-fast modified Leslie–Gower model

B. Ambrosio*,[a], M.A. Aziz-Alaoui[a], R. Yafia[b]

[a] Normandie Univ, UNIHAVRE, LMAH, FR-CNRS-3335, ISCN, 76600 Le Havre, France
[b] Ibn Zohr University, Agadir, Morocco

ARTICLE INFO

Keywords:
Dynamical systems
Prey-Predator models
Slow-fast analysis
Canards

ABSTRACT

Geometrical Singular Perturbation Theory has been successful to investigate a broad range of biological problems with different time scales. The aim of this paper is to apply this theory to a predator-prey model of modified Leslie–Gower type for which we consider that prey reproduces mush faster than predator. This naturally leads to introduce a small parameter ϵ which gives rise to a slow-fast system. This system has a special folded singularity which has not been analyzed in the classical work [15]. We use the blow-up technique to visualize the behavior near this fold point P. Outside of this region the dynamics are given by classical regular and singular perturbation theory. This allows to quantify geometrically the attractive limit-cycle with an error of $O(\epsilon)$ and shows that it exhibits the *canard* phenomenon while crossing P.

1. Biological motivation and formulation of the model

In [17], see also [18], Leslie introduced the following prey-predator model:

$$\begin{cases} \dot{x} &= (r_1 - b_1 x - a_1 y)x, \\ \dot{y} &= \left(r_2 - a_2 \frac{y}{x}\right)y \end{cases} \tag{1}$$

The first equation, which describes the evolution of the prey, has a logistic term, $r_1 x - b_1 x^2$, standing for growth under limited quantity of food, as well as a classical Lotka–Volterra term, $- a_1 xy$ for the mortality due to predation. More surprising is the term $-a_2 \frac{y^2}{x}$ instead of the classical Lotka–Volterra term $+ a_2 xy$ or a logistic term $- a_2 y^2$, appearing in the equation for the predator y. Leslie introduced it, to fit data on growth of Paramedum Caudatum and Paramecium Aurelia cultures, in which the food supply consisted of a suspension of Bacillus Pyocyaneus in a buffered medium. It appeared that to fit data, the constant in front of the term $- y^2$ in the classical logistic term, should be inversely proportional to the concentration of food. That was the argument which originally led Leslie to introduce the term $-a_2 \frac{y^2}{x}$.

A slightly improvement of this model, came with the following equation which appeared in [27], and which we call, following [22], the Holling–Tanner model:

$$\begin{cases} \dot{x} = \left(r_1 - b_1 x - \frac{a_1 y}{x + k_1}\right)x, \\ \dot{y} = \left(r_2 - \frac{a_2 y}{x}\right)y \end{cases} \tag{2}$$

The difference with the previous equation is that the term $- a_1 yx$ is replaced by the Holling functional response of type II, $- \frac{a_1 y}{x + k_1} x$. Recall that, in [11], see also [9,10], Holling gives several examples of prey and predator populations in which the response of predators as function of prey density is classified into three types. For example, the functional response of type II is found to fit the data of populations of Mantids Hierodula crassa (predator) and houseflies (prey) put together in a cage, see [11]. Related mathematical aspects of these models can also be found in [14,19,23].

More recently, in [1], see also [20,21], Alaoui and Okiye introduced the following model:

$$\begin{cases} \dot{x} = \left(r_1 - b_1 x - \frac{a_1 y}{x + k_1}\right)x, \\ \dot{y} = \left(r_2 - \frac{a_2 y}{x + k_2}\right)y \end{cases} \tag{3}$$

The difference with the previous model is the constant k_2. It was first introduced to avoid a mathematical singularity at $x = 0$. From a biological point of view, in case of severe scarcity of prey, adding a positive constant to the denominator, introduces a maximum decrease rate, which stands for environment protection. There is a wide variety of natural systems which may be modeled by system (3), see [7,20,21,28]. It may, for example, be considered as a representation of an insect pest-

* Corresponding author.
E-mail address: benjamin.ambrosio@univ-lehavre.fr (B. Ambrosio).

https://doi.org/10.1016/j.mbs.2017.11.003
Received 3 April 2017; Received in revised form 14 September 2017; Accepted 1 November 2017

spider food chain. Let us give more details on the model parameters; r_1, r_2, a_1, a_2, b_1, k_1 and k_2 are assumed to be positive. They are defined as follows: r_1 (resp. r_2) is the growth rate of prey x (resp. predator y), b_1 measures the strength of competition among individuals of species x, a_1 (resp. a_2) is the maximum value of the per capita reduction rate of x (resp. y) due to y, k_1 (respectively, k_2) measures the extent to which environment provides protection to prey x (respectively, to the predator y). In order to simplify (3), we proceed to the following change of variables:

$u(r_1 t) = \frac{b_1}{r_1} x(t), v(r_1 t) = \frac{a_2 b_1}{r_1 r_2} y(t), a = \frac{a_1 r_2}{a_2 r_1}, \epsilon = \frac{r_2}{r_1}, e_1 = \frac{b_1 k_1}{r_1}, e_2 = \frac{b_1 k_2}{r_1}$, $t' = r_1 t$.

For convenience, we drop the primes on t. We obtain the following system:

$$\begin{cases} u_t &= u(1-u) - \frac{auv}{u+e_1}, \\ v_t &= \epsilon v\left(1 - \frac{v}{u+e_2}\right). \end{cases} \tag{4}$$

We assume here that the prey reproduces much faster than the predator, *i.e.* $r_1 > > r_2$, which implies that ϵ is small. This will allow us to use slow-fast analysis which simplifies the analysis by discriminating between slow and fast trajectories.

2. Characterization of the attractive limit-cycle

We first note that there are special solutions to Eq. (4): $u = 0$, $v_t = \epsilon v\left(1 - \frac{v}{e_2}\right)$ and $v = 0$, $u_t = u(1-u)$. Hence, the quadrant $(0 \le u \le 1, v \ge 0)$ is positively invariant for (4). We restrict our analysis to this quadrant. We also assume the following conditions which ensure the existence of a unique attractive limit-cycle for (4):

$ae_2 < e_1$, ae_2 not to close of e_1,

and,

$u^* < \frac{1-e_1}{2}$, u^* not to close of $\frac{1-e_1}{2}$,

where u^* is solution of

$u + e_2 = g(u)$,

and:

$g(u) = \frac{1}{a}(1-u)(u+e_1)$.

Under these assumptions, there are four fixed points in the positive quadrant:

$P_1 = (0,0)$, $P_2 = (0, e_2)$, $P_3 = (1, 0)$, $P_4 = (u^*, g(u^*))$.

We will see that condition $0 < u^* < \frac{1-e_1}{2}$ ensures that P_4 belongs to the repulsive part of $v = g(u)$, whereas the condition $e_2 < \frac{e_1}{a}$ implies that P_2 lies on the repulsive part of the v axis.

These conditions also prevent additional singularities for the folded points. Fig. 2 illustrates nullclines and the attractive limit-cycle for (4). Our aim is to characterize the limit-cycle. The first step, is to proceed to the classical slow-fast analysis. It is of fundamental importance and will be detailed in Section 3. It provides an efficient geometrical description of the dynamics and can be summarized trough the observation of Fig. 2. Indeed, this figure gives the main dynamics of the system. Basically, outside of a neighborhood of the nullcline $u(1-u) - a\frac{uv}{u+e_1} = 0$, (*i.e.* $u = 0$ or $v = g(u)$ with $g(u) = \frac{1}{a}(u+e_1)(1-u)$), the trajectories are horizontal and their direction are given by the sign of $1 - u - \frac{av}{u+e_1}$. Let $\mathscr{C}$ the representative curve of g in the positive quadrant (in green in Fig. 2). When the trajectories reach the right part of $\mathscr{C}$, they remain stuck there, and grow slowly, until they reach a fold (the point D). Then, they jump to the manifold $u = 0$. There, the trajectories remain stuck again until they are repelled after crossing a fold point. However, near this special fold point, the classical analysis fails. We will call it P. The blow-up technique is naturally introduced in the fourth section, to analyze the trajectories near P. The blow-up technique is a clever change of variables, see [4,5,15]. Hence, in our article, the dynamics of system (4) are described thanks to:

- classical slow-fast analysis and geometrical, regular and singular, perturbation theory outside of a neighborhood of P,
- blow-up technique in a neighborhood of P.

These techniques allow to quantify the limit-cycle which attracts all the trajectories of the positive quadrant. Now, we introduce some notations to quantify the limit-cycle.

We fix a small value $\alpha > 0$ and define a cross section . This means that V intersects the y axis just above the intersection of $\mathscr{C}$ and the y axis. By the regularity of the flow with regard to ϵ, the limit cycle will cross V at a point $(k(\alpha)\epsilon + o(\epsilon), \frac{e_1}{a} + \alpha)$, with $k(\alpha) > 0$ (below, for convenience, we do not write the dependence on α). We now introduce some notations which will be used throughout the article. Let

$$\overline{u} = \frac{1-e_1}{2},$$

and

$$A = (0, g(\overline{u})),\ B = \left(0, \frac{e_1}{a} + \alpha + \frac{c_2}{c_1 k}\right),\ C = \left(u_*, \frac{e_1}{a} + \alpha + \frac{c_2}{c_1 k}\right),\ D = (\overline{u}, g(\overline{u})),$$

where u_* is such that $g(u_*) = \frac{e_1}{a} + \alpha + \frac{c_2}{c_1 k}$ and

$$c_1 = \frac{1-e_1}{e_1},\ c_2 = \frac{e_1}{a}\left(1 - \frac{e_1}{a e_2}\right).$$

Note that $c_1 > 0$, whereas $c_2 < 0$. This implies that B is under P, which will be important regarding the existence of canard solutions. Let γ' be the closed curve defined by:

$\gamma' = [A, B] \cup [B, C] \cup \zeta \cup [D, A]$

where,

$\zeta = \{(u, g(u));\ \overline{u} \le u \le u_*\}$.

The following result holds.

Theorem 1. *All the trajectories not lying in* $u = 0$ *and* $v = 0$, *and different from the fixed point* P_4, *evolve asymptotically towards a unique limit-cycle* γ *which is* $O(\epsilon)$ *close of* γ'.

Proof. The existence of the cycle results from Poincare–Bendixon theorem. For uniqueness, we refer to [2]. The approximation by γ' results from slow-fast analysis and the blow-up technique which will be carried out in Sections 2 and 3. □

Remark 1. According to [3,15,26], the canard phenomenon occurs when a trajectory crosses a folded point from the attractive manifold and follows the repulsive manifold during a certain distance before being repelled away. We will see that according to this definition, the canard phenomenon occurs here. That is why we have introduced α and k. Another way to express this comes with the following argument: for those who are somehow familiar with slow-fast analysis, the first naive interpretation which comes in mind after the computation of critical manifolds, is to believe that the limit-cycle leaves the manifold $u = 0$ at a jump point, when the manifold u becomes unstable. In fact, this is not the case, the trajectory follows the unstable manifold until reaching B as our theoretical analysis as well as numerical simulations show.

Remark 2. We can try to interpret the slow-fast attracting limit-cycle in the prey-predator modeling context. For a time large enough, the dynamics of populations follow the cycle. If we start on the cycle close to the point A, there is near zero quantity of prey u, and a certain

quantity of predator v. Since there is no prey, the quantity of predator decreases. It decreases quite slowly, along the slow manifold (this geometrical expression will be detailed in the next section), until it reaches the point B. There, due to the low quantity of predator and the fast reproduction of prey (i.e. due to the ϵ of the u derivative), a very fast increase in the prey population occurs. It corresponds to the time at which the trajectory leaves the slow manifold. The predator population do not increase during this short time, it remains near constant (this is a jump in u). When the prey reaches a region (a neighborhood of C), where its derivative is zero i.e. another part of the slow manifold (related with the first Holling–Tanner equation), the increase of u stops. Then, there is enough preys to induce an increase in the predator population. In the meantime, as the predator population increases, the prey population decreases. This is a slow process which occurs all along the slow manifold: the relation between u and v are given by the slow-manifold equation. This remains true until the trajectories reach the fold of the slow manifold (the point D), again given by the Holling–Tanner profile. There, due to the fold, the prey population decreases quickly while the predator remain near constant (this is another jump in u). The trajectories reach the region near the point A and the scenario is repeated. Basically, we can summarize the process as follows:

1. When the quantity of prey is near zero, the quantity of predator decreases. This is a slow process along the left part of the slow manifold.
2. When the predator population is below a threshold, the trajectory leaves the left slow manifold. There is a quick increase in prey, this is a fast process, a jump. And the trajectory reaches the right slow manifold.
3. The prey population is now large. The predator population starts to increase. As the predator population increases, the prey population decreases. This occurs along the slow manifold. The prey and predator populations are related by the slow manifold equation. This is a slow process.
4. When the trajectory reaches the fold, which corresponds to a threshold in predator population and its related prey population along the slow manifold, there is a quick decrease in the prey population. This is again a fast process, a jump. The trajectory reaches the near zero quantity of prey, which corresponds to the right part of the slow manifold. The loop is closed (4).

See Figs. 1,2,3,4 and 5, for illustrations of the process.

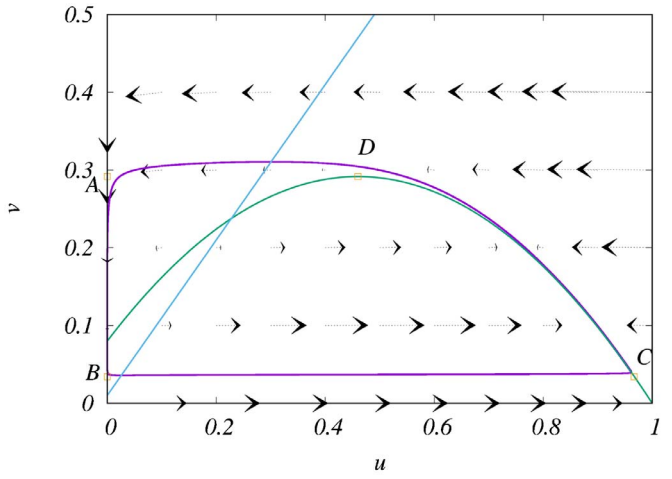

Fig. 1. Limit cycle and nullclines of system (4) for $a = 1$, $e_1 = 0.08$,$e_2 = 0.01$ and $\epsilon = 0.01$.

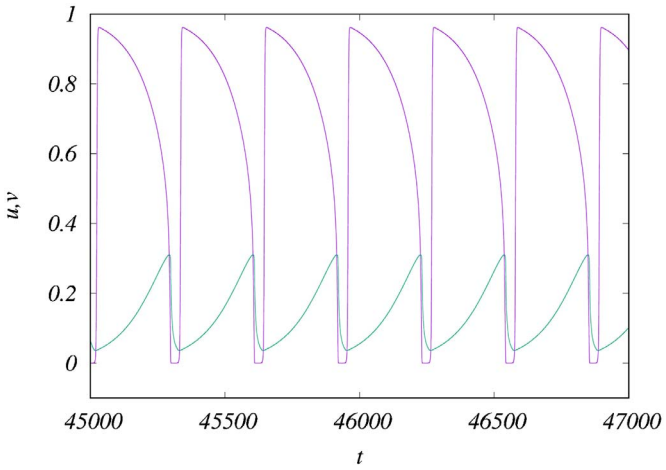

Fig. 2. Limit cycle of system (4) for $a = 1$, $e_1 = 0.08$,$e_2 = 0.01$ and $\epsilon = 0.01$. We represent the preys u, in purple, and the predators, in green, as functions of time. (For interpretation of the references to color in this figure legend, the reader is referred to the web version of this article.)

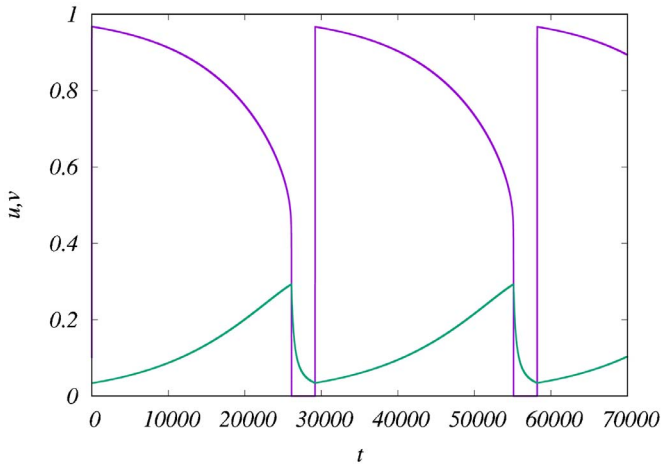

Fig. 3. Limit cycle of system (4) for $a = 1$, $e_1 = 0.08$,$e_2 = 0.01$ and $\epsilon = 0.0001$. We represent the preys u, in purple, and the predators, in green, as functions of time. (For interpretation of the references to color in this figure legend, the reader is referred to the web version of this article.)

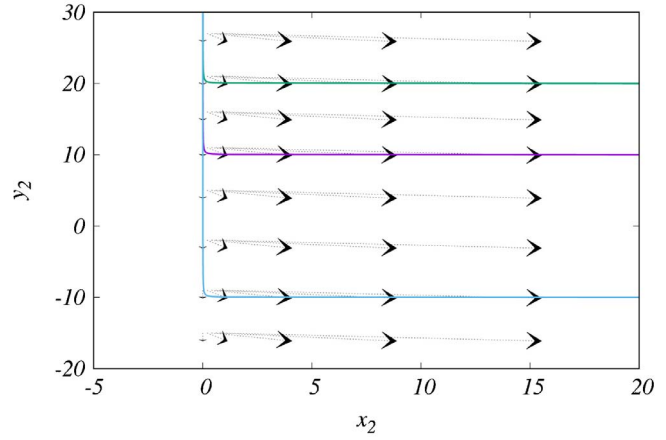

Fig. 4. Vector field and three orbits solutions of system (18) (chart K_2) for $a = 1$, $e_1 = 0.08$, and $e_2 = 0.01$. These solutions are defined on the time interval $]-\infty;\frac{1}{c_1 x_2(0)}[$. According with Proposition 3, we observe that $x_2 = 0$ is a vertical asymptote for each of them while they have a distinct horizontal asymptote.

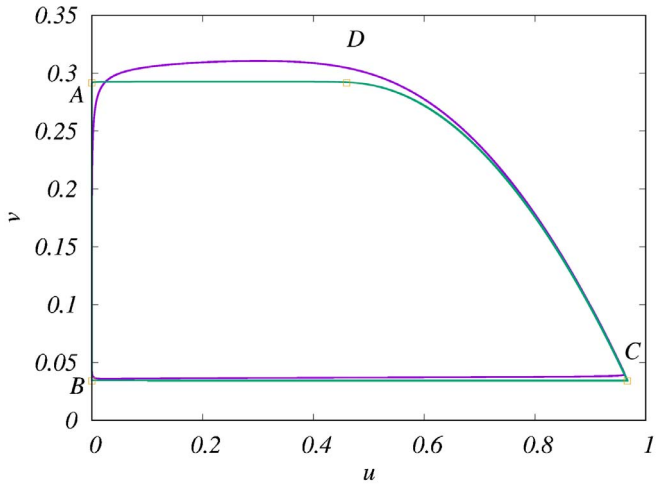

Fig. 5. Solutions of system (4) with $a = 1$, $e_1 = 0.08$, and $e_2 = 0.01$. Limit-cycles for $\epsilon = 10^{-2}$ in purple and $\epsilon = 10^{-4}$ in green. As ϵ approaches 0 the limit-cycle approaches γ'. Choosing $\alpha = 0$, we obtain an approximate value of $k \simeq -\frac{c_2}{Dc_1}$ where D is the distance between the coordinate of the fast-fiber followed by the limit cycle and $\frac{e_1}{a}$. Here, we find $D \simeq 0.045$ and $k \simeq 1.086$, ($c_1 = 11.5$, $c_2 = -0.56$). This means that the limit-cycle crosses the axis $v = \frac{e_1}{a}$ at a value $1.086\epsilon + o(\epsilon)$. (For interpretation of the references to color in this figure legend, the reader is referred to the web version of this article.)

3. Slow-Fast analysis

In this section, we proceed to a classical slow-fast analysis, see for example [6,8,12,13,15]. We study the layer system and the reduced system. The layer system is obtained by setting $\epsilon = 0$ in system (4). It reads as,

$$\begin{cases} u_t &= u(1-u) - \frac{auv}{u+e_1} = F(u,v), \\ v_t &= 0. \end{cases} \tag{5}$$

The stationary points of this system are given by:

$$M_0 = \left\{ u = 0 \text{ or } v = \frac{1}{a}(1-u)(u+e_1) = g(u) \right\}. \tag{6}$$

The set M_0 is called the critical manifold. Outside from a neighborhood of this manifold, for ϵ small, regular perturbation theory ensures that trajectories of system (4) are $O(\epsilon)$-close to those of system (5). The trajectories of system (5) are tangent to the u-axis, which justifies the name of "layer system". These trajectories are the fast trajectories. Furthermore, the Fenichel theory, see [6] or references cited above, provides the existence of a locally invariant manifold M_ϵ, $O(\epsilon)$-close to the critical manifold M_0 for compact subsets of M_0 where $F'_u(u,v) \neq 0$. The system will follow the fast trajectories outside of this manifold. We have to evaluate $F'_u(u,v)$ on the critical manifold. The parts of M_0 where $F'_u(u,v) < 0$ is called the attractive part of the critical manifold. Analogously, the part of M_0 where $F'_u(u,v) > 0$ is called the repulsive part of the critical manifold. Now, we compute these subsets of M_0. We start our computations with the case $u = 0$. We have,

$$F'_u(0,v) = 1 - \frac{av}{e_1}. \tag{7}$$

Therefore,

$$F'_u(0,v) > 0 \Leftrightarrow v < \frac{e_1}{a}. \tag{8}$$

Now, we deal with the case $v = g(u) = \frac{1}{a}(1-u)(u+e_1)$. We have

$$F'_u(u,v) = 1 - 2u - av\frac{e_1}{(u+e_1)^2}. \tag{9}$$

For $v = g(u)$, we obtain,

$$F'_u(u,v) = \frac{u}{u+e_1}(-2u + (1-e_1)). \tag{10}$$

Therefore,

$$F'_u(u,g(u)) > 0 \Leftrightarrow u < \frac{1-e_1}{2} = \overline{u}. \tag{11}$$

Finally, the attractive critical manifold $M_{0,\,a}$ is given by $u = 0$ and $v > \frac{e_1}{a}$, or $v = g(u)$ and $\frac{1-e_1}{2} < u \leq 1$:

$$M_{0,a} = \left\{ (0,v);\, v > \frac{e_1}{a} \right\} \cup \left\{ (u, g(u));\, \frac{e_1}{a} < u \leq 1 \right\}.$$

Analogously, the repulsive critical manifold $M_{0,\,r}$ is given by:

$$M_{0,r} = \left\{ (0,v);\, 0 \leq v < \frac{e_1}{a} \right\} \cup \{ (u, g(u));\, 0 \leq u < \overline{u} \}.$$

The non-hyperbolic points of the critical manifold, or fold points, where $F'(u,v) = 0$ are $P = (0, \frac{e_1}{a})$ and $D = (\overline{u}, g(\overline{u}))$. Now, we look at the reduced system. The reduced system gives the slow-trajectories *i.e.*, the trajectories within the critical manifold which persists for ϵ small within the locally invariant manifold M_ϵ. It is obtained by setting $\epsilon = 0$ after the change of time $\tau = \epsilon t$ in (4). It reads as (to avoid complications, we keep the notation with t, but it should be with τ),

$$\begin{cases} 0 &= u(1-u) - \frac{auv}{u+e_1}, \\ v_t &= v\left(1 - \frac{v}{u+e_2}\right). \end{cases} \tag{12}$$

For $u = 0$, we obtain,

$$v_t = v\left(1 - \frac{v}{e_2}\right). \tag{13}$$

This implies that

$$v_t > 0 \Leftrightarrow v < e_2.$$

Note that $(0, e_2)$ are the coordinates of the fixed point P_2 of the original system.

In the other part of the critical manifold, *i.e.* for $v = g(u)$, we have

$$\begin{aligned} & v_t > 0 \\ \Leftrightarrow\ & v\left(1 - \frac{v}{u+e_2}\right) > 0 \\ \Leftrightarrow\ & v < u + e_2. \end{aligned}$$

Also, using the second equation of (12) $v_t = g'(u)u_t$, we find,

$$v_t = g'(u)u_t = g(u)\left(1 - \frac{g(u)}{u+e_2}\right).$$

Therefore,

$$u_t = \frac{g(u)}{g'(u)}\left(1 - \frac{g(u)}{u+e_2}\right).$$

The points where $g' = 0$ correspond to a jump-point if $g(u) \neq u + e_2$, since in this case, we have formally at this point, $u_t = -\infty$. The analysis of the layer and the reduced system give the qualitative behavior of the system outside of the neighborhood of the fold-points. Trajectories reach the slow attractive manifold, and follow it according to the dynamics, or are repelled by the repulsive slow manifold. Furthermore, the behavior near the jump-point $(\overline{u}, g(\overline{u}))$, has been rigorously described in [15]. Trajectories reaching a neighborhood of the fold point from the right exit the neighborhood at left along fast fibers, and there is a contraction of rate $e^{-\frac{c}{\epsilon}}$ for some constant c between arriving and exiting trajectories. The Fig. 2 illustrates this behavior. Therefore, it remains only to analyze the behavior of trajectories near the fold point $P = (0, \frac{e_1}{a})$. This is the point we deal with, in the next section, thanks to the blow-up technique. Note that this has not been done in [15] since it is assumed there that critical manifold can be written $v = \varphi(u)$ with $\varphi'(0) = 0$ and $\varphi''(0) \neq 0$, which is not the case here since M_0 writes

$u = 0$ in a neighborhood of the fold-point $P = (0, \frac{e_1}{a})$.

Remark 3. Canards may appear near the fold point $D = (\overline{u}, g(\overline{u}))$, when

$$g(u) \simeq u + e_2. \tag{14}$$

As we have already mentioned, canards are solutions that follow the repulsive manifold during a certain distance after crossing the fold before being repelled. They have been discovered by French mathematicians with non standard analysis and studied after with geometrical singular perturbation theory, see [3,15,26]. Our assumptions prevent the apparition of canards near D. Near $P = (0, \frac{e_1}{a})$, the limit-cycle exhibit the canard phenomenon as it is stated in Theorem 1, since it is repelled by the slow repulsive manifold only within a region $O(\epsilon)$ close of B, which is above P. The condition $e_2 \simeq \frac{e_1}{a}$, which is the analog of (14) for P would lead to higher singularity. We do not consider this case here.

4. Blow-up technique near the fold-point $P = (0, \frac{e_1}{a})$.

In this section, we deal with the blow-up technique which gives the dynamics near the fold point and provides the final argument for the proof of Theorem 1. First, in Proposition 1, we rewrite Eq. (4) with local coordinates around P. Then, we compute the blow-up. The blow-up may be seen as a zoom, which allows a de-singularization near the fold point. We will focus only in the chart called K_2. Propositions 2–4 detail the dynamics on this chart. Then, we prove Theorem 1. For this, we need to compute the y-coordinate at which the limit-cycle leaves the left repulsive slow manifold. Remark 4 gives first the intuition of the proof which immediately follows. It relies directly on the solution computed explicitly in chart K_2. Finally, the last remark of the section makes the link with existing works. The following proposition gives the formulation of Eq. (4), when written around $P = (0, \frac{e_1}{a})$:

Proposition 1. *Near the fold point* $P = (0, \frac{e_1}{a})$, *system (4) rewrites:*

$$\begin{aligned}
\dot{x} &= c_1 x^2 - \tfrac{a}{e_1} xy + O(\|(x,y)\|^3)\Big) \\
\dot{y} &= \epsilon(c_2 + \tfrac{e_1^2}{a^2 e_2^2} x + \Big(1 - \tfrac{2e_1}{ae_2}\Big) y + O(\|(x,y)\|^2)) \\
\dot{\epsilon} &= 0
\end{aligned} \tag{15}$$

where

$$c_1 = \frac{1 - e_1}{e_1},\ c_2 = \frac{e_1}{a}\Big(1 - \frac{e_1}{ae_2}\Big).$$

Proof. Classically, the constant ϵ is first turned into a variable of the system by setting $\dot{\epsilon} = 0$. Then we proceed with the change of variables

$$u = x,\ v = \frac{e_1}{a} + y.$$

Plugging into (4) gives:

$$\begin{aligned}
\dot{x} &= x(1-x) - a\tfrac{x}{e_1 + x}\Big(\tfrac{e_1}{a} + y\Big) \\
\dot{y} &= \epsilon\Big(\tfrac{e_1}{a} + y\Big)\Big(1 - \tfrac{e_1}{a(x + e_2)} - \tfrac{y}{x + e_2}\Big) \\
\dot{\epsilon} &= 0.
\end{aligned}$$

Then, we use the following Taylor development:

$$\frac{1}{e_1 + x} = \frac{1}{e_1} - \frac{1}{e_1^2} x + \frac{1}{e_1^3} x^2 + o(x^2).$$

We find,

$$\begin{aligned}
\dot{x} &= \Big(\tfrac{1}{e_1} - 1\Big)x^2 - \tfrac{a}{e_1} xy + O(x^3) + O(x^2 y) \\
\dot{y} &= \epsilon(\tfrac{e_1}{a}\Big(1 - \tfrac{e_1}{ae_2}\Big) + \tfrac{e_1^2}{a^2 e_2^2} x + \Big(1 - \tfrac{2e_1}{ae_2}\Big) y + O(\|(x,y)\|^2)) \\
\dot{\epsilon} &= 0,
\end{aligned} \tag{16}$$

which gives the result. □

We will now apply the blow-up technique. Here, the blow-up technique consists in a local change of variables, from $\mathbb{R}^3$ into $\mathbb{R}^4$, which allows to de-singularize the fold-point and visualize the trajectories in different charts. We use the following change of variables:

$$x = \overline{r}\overline{x},\ y = \overline{r}^2 \overline{y},\ \epsilon = \overline{r}^3 \overline{\epsilon}.$$

Note that the analysis will be done for $\overline{r}$ small. Hence, this change of variables is a kind of zoom, with different weights (1,2 and 3), around the point (0, 0, 0). If the x, y and z were very small near the origin, the $\overline{x}$, $\overline{y}$ and $\overline{z}$ do not need to be small anymore. Moreover, the weights chosen here are good for our computations and will allow to visualize the trajectories when they cross the fold point. These weights are taken from [15]. For a general description of blow-up methods, see [4]. For applications to the canards in the paradigmatic Van Der Pol equation, see [5]. Here, the computation gives (we drop the bar):

$$\begin{aligned}
\dot{r}x + r\dot{x} &= c_1 r^2 x^2 - \tfrac{a}{e_1} r^3 xy + O(r^4 x^2 y) + O(r^3 x^3) \\
2ry\dot{r} + r^2\dot{y} &= r^3\epsilon(c_2 + \tfrac{e_1^2}{a^2 e_2^2} rx + \Big(1 - \tfrac{2e_1}{ae_2}\Big) r^2 y + O(\|(rx, r^2 y)\|^2)) \\
3r^2\epsilon\dot{r} + r^3\dot{\epsilon} &= 0
\end{aligned}$$

Classically, see [15] and references therein, the chart K_1 is obtained by setting $\overline{y} = 1$. The chart K_2 is obtained by setting $\overline{\epsilon} = 1$. The chart K_3 is obtained by setting $\overline{x} = 1$. Hence, choosing a particular chart, means that we focus in a particular region of the new coordinate system. In this paper, we only consider the chart K_2. It will be fundamental in our analysis, and will allow to prove Theorem 1. Since we work in chart K_2, according to classical notations, we use the subscript 2.

Dynamics in chart K_2.

Proposition 2. *The dynamics in chart* K_2 *are given by the system:*

$$\begin{aligned}
\dot{x}_2 &= c_1 x_2^2 + O(r_2)) \\
\dot{y}_2 &= c_2 + O(r_2) \\
\dot{r}_2 &= 0
\end{aligned} \tag{17}$$

Proof. Setting $\overline{\epsilon} = 1$ in (4) gives:

$$\begin{aligned}
\dot{x}_2 &= r_2(c_1 x_2^2 + O(r_2)) \\
\dot{y}_2 &= r_2(c_2 + O(r_2)) \\
\dot{r}_2 &= 0.
\end{aligned}$$

Then, we perform the change of time $\tau = r_2 t$. This gives:

$$\begin{aligned}
r_2\dot{x}_2 &= r_2(c_1 x_2^2 + O(r_2)) \\
r_2\dot{y}_2 &= r_2(c_2 + O(r_2)) \\
\dot{r}_2 &= 0.
\end{aligned}$$

Which by dividing by r_2 gives the result. □

This computation is an essential key of our blow-up. The last change of time and the division by r_2 has allowed to blow-up the dynamics. Here occurs the de-singularization. We can now visualize how the trajectories behave when crossing the fold. For $r_2 = 0$, we obtain:

$$\begin{aligned}
\dot{x}_2 &= c_1 x_2^2 \\
\dot{y}_2 &= \tfrac{e_1}{a}\Big(1 - \tfrac{e_1}{ae_2}\Big) \\
\dot{r}_2 &= 0.
\end{aligned} \tag{18}$$

Proposition 3. *The solution of system (18) is:*

$$\begin{aligned} x_2(t) &= \frac{1}{x_2^{-1}(0) - c_1 t} \\ y_2(t) &= y_2(0) + c_2 t \end{aligned} \tag{19}$$

i.e.

$$x_2(t) = \frac{1}{x_2^{-1}(0) - c_1 \frac{y_2(t) - y_2(0)}{c_2}}$$

or

$$y_2(t) = y_2(0) + \frac{c_2}{c_1}\left(\frac{1}{x_2(0)} - \frac{1}{x_2(t)}\right)$$

It follows that orbits have the following properties:

1. *Every orbit has a horizontal asymptote* $y = y_r$, *where* y_r *depends on the orbit such that* $x \to +\infty$ *as* y *approaches* y_r *from above.*
2. *Every orbit has a vertical asymptote* $x = 0^+$.
3. *The point* $(x_2(0), \alpha, 0)$ *is mapped to the point* $\left(\delta, \alpha + \frac{c_2}{c_1}\left(\frac{1}{x_2(0)} - \frac{1}{\delta}\right)\right)$.

Proof. It follows easily from the explicit solution. □

Proposition 4. *Solutions of (17) are* $O(r)$*-close of those of (18).*

Proof. This follows from regular perturbation theory. □

Remark 4. Let us make a remark on the first statement of Proposition 3. For $t^* = \frac{1}{c_1 x_2(0)}$, x_2 blows-up. Since $x_2 = \frac{x}{r_2}$, and $r_2 = \epsilon^{\frac{1}{3}}$, $x_2 = +\infty$ correspond, when $\epsilon = 0$ to a point $x > 0$ where we can consider that trajectory has left the neighborhood of the fold and where the previous slow-fast analysis applies. This gives for y_2:

$$y_2(t^*) = y_2(0) + \frac{c_2}{c_1 x_2(0)}. \tag{20}$$

This means, that fixing $x_2(0)$ and $y_2(0)$, the value where the trajectory leaves the slow manifold and connects the fast fiber is determined by (20). Therefore, if we choose $(x_2(0), y_2(0))$ on the limit-cycle, this determines the fast fiber followed by the limit-cycle. We will now detail this argument which gives the proof of Theorem 1.

Proof of Theorem 1. Fix a value x far from 0, let's say $x = \frac{1}{2}$. We want to determine t^* such that $x(t^*) = \frac{1}{2}$, which corresponds to $x_2(t^*) = \frac{1}{2\epsilon^{\frac{1}{3}}}$. Taking $x(0) = k\epsilon + o(\epsilon)$, and according to equation (19), this gives:

$$t^* = \frac{\epsilon^{\frac{1}{3}}}{c_1}\left(\frac{1}{k\epsilon + o(\epsilon)} - 2\right)$$

and for Eq. (17),

$$y_2(t^*) = y_2(0) + \frac{c_2 \epsilon^{\frac{1}{3}}}{c_1}\left(\frac{1}{k\epsilon + o(\epsilon)} - 2\right) + O(\epsilon),$$

which in original coordinates gives:

$$y(t^*) = y(0) + \frac{c_2}{k c_1} + O(\epsilon).$$

This proves the theorem. □

Remark 5. Note that the folded node P is at the intersection of the two branches of the manifold M_0, $v = g(u)$ and $u = 0$. Note also that these two branches actually exchange their stability at P. This case has been treated in a general form in [16] under the appropriate name of transcritical bifurcation. However, here, we are precisely in the special case $\lambda = 1$ excluded from theorem 2.1 of [16]. Indeed, using the notations of this article, we can compute from Eq. (16):

$$\begin{aligned} &\alpha = \frac{1}{e_1} - 1, \quad \beta = -\frac{e_1}{a} \quad g_0 = \frac{e_1}{a}\left(1 - \frac{e_1}{e_2}\right) \\ &\gamma = 0 \qquad\qquad \delta = 0 \end{aligned} \tag{21}$$

and

$$\lambda = \frac{\delta\alpha + g_0\beta}{|g_0|\sqrt{\beta^2 - \gamma\alpha}} = \frac{g_0\beta}{|g_0||\beta|} = 1. \tag{22}$$

The authors have announced the existence of the canard in this case without giving the detailed proof of it. Here, we have proved the canard phenomenon using the blow up technique in the case of the limit-cycle of this classical model of predator-prey.

Remark 6. Close phenomena have been analysed in [24,25] for prey-predator and population models with different techniques.

Comments on numerical methods

The computation of solutions have been performed using the Runge–Kutta 4 method in our own $C++$ program. Note that to compute solutions of Fig. 3, we have started with final condition and computed backward trajectories. This was to avoid the difficulty of the sensitivity of initial conditions near the manifold $u = 0$.

5. Conclusion

In this article, we have characterized the limit-cycle of the system (4). The system was originally introduced in [1] as a modification of the Leslie–Gower model. We have proved that the limit-cycle of the model exhibits the canard phenomenon when crossing a special folded node. We have also computed the value at which it reaches the fast fiber. In a forthcoming work, we hope to investigate the diffusive model obtained by adding a Laplacian term in the first equation.

Acknowledgments

We would like to thank Region Normandie France and the ERDF (European Regional Development Fund) project XTERM (previously RISK). We also thank N. Popovic for some relevant remarks.

Supplementary material

Supplementary material associated with this article can be found, in the online version, at 10.1016/j.mbs.2017.11.003.

References

[1] M.A. Aziz-Alaoui, M.D. Okiye, Boundedness and global stability for a predator-prey model with modified Leslie–Gower and Holling-type *II* schemes, Appl. Math. Lett. 16 (2003) 1069–1075.
[2] M.D. Okiye, Étude et analyse asymptotique de certains systèmes dynamiques non-linéaires: application à des problèmes proie-prédateurs. Phd thesis, Le Havre, 2004.
[3] E. Benoit, J.-L. Callot, F. Diener, M. Diener, Chasse au canards, Collect. Math. 31–32 (1981) 37–119.
[4] F. Dumortier, Techniques in the theory of local bifurcations: blow-up, normal forms, nilpotent bifurcations, singular perturbations, in: D. Szlomiuk (Ed.), Bifurcations and Periodic Orbits of Vector Fields, Kluwer, Dordrecht, The Netherlands, 1993, pp. 19–73. NATO Adv. Sci. Inst. Ser. C Math. Phys. Sci. 408.
[5] F. Dumortier, R. Roussarie, Canard cycles and center manifolds, Memoirs of the American Mathematical Society, 577 Providence, 1996.
[6] N. Fenichel, Geometric singular perturbation theory for ordinary differential equations, J. Differ. Equ. 31 (1979) 53–98.
[7] I.L. Hanski, L. Hassen, H. Huttonen, Specialist predation, generalist predation and the rodent microtine cycle, J. Anim. Ecol. 60 (1991) 353–367.
[8] G. Hek, Geometric singular perturbation theory in biological practice, J. Math. Biol. 60 (2010) 347–386.
[9] C.S. Holling, The Components of Predation as Revealed by a Study of Mammal Predation of the European Pine Sawfly, The Canadian Entomologist, XCI, 1959, pp. 293–320.
[10] C.S. Holling, Some Characteristics of Simple Type of Predation and Parallelism, The Canadian Entomologist, XCI, 1959, pp. 385–398.
[11] C.S. Holling, The functional response of predators to prey density and its role in mimicry and population regulation, Memoirs of the Entomological Society of Canada, 45 (1965), pp. 3–60.
[12] C.K.R.T. Jones, Geometric singular perturbation theory, in: R. Johnson (Ed.), Dynamical Systems, Lecture Notes in Mathematics, Springer, Montecatibi Terme, Berlin, 1995, pp. 44–118. 1609.
[13] T.J. Kaper, An introduction to geometric methods and dynamical systems theory for

singular perturbation problems, in: J. Cronin, Jr R. E OMalley (Eds.), Analyzing Multiscale Phenomena Using Singular Perturbation Methods, Providence, 56, 1999, pp. 85–132. Proc Symposia Appl Math, AMS.
[14] A. Korobeinikov, A Lyapunov function for Leslie-Gower predator-prey models, Appl. Math. Lett. 14 (2001) 697–699.
[15] M. Krupa, P. Szmolyan, Extending geometric singular perturbation theory to non-hyperbolic points-fold and canard points in two dimensions, SIAM J. Math. Anal. 33 (2001) 286–314.
[16] M. Krupa, P. Szmolyan, Extending slow manifolds near transcritical and pitchfork singularities, Nonlinearity 14 (2001) 1473–1491.
[17] P.H. Leslie, Some further notes on the use of matrices in population mathematics, Biometrika 35 (1948) 213–245.
[18] P.H. Leslie, J.C. Gower, The properties of a stochastic model for the predator-prey type of interaction between two species, Biometrika 47 (1960) 219–234.
[19] R.M. May, Stability and Complexity in Model Ecosystems, NJ: Princeton University Press, Princeton, 1973.
[20] A.F. Nindjin, M.A. Aziz-Alaoui, M. Cadivel, Analysis of a predatorprey model with modified Leslie-Gower and Holling-type II schemes with time delay, Nonlinear Anal. Real World Appl. 7 (2006) 1104–1118.
[21] A.F. Nindjin, M.A. Aziz-Alaoui, Persistence and global stability in a delayed Leslie-Gower type three species food chain, J. Math. Anal. Appl. 340 (2008) 340–357.
[22] E.C. Pielou, Mathematical Ecology, John Wiley and Sons, New York, 1977.
[23] M.L. Rosenzweig, R.H. MacArthur, Graphical representation and stability conditions of predatorprey interaction, Amer. Naturalist. 47 (1963) 209–223.
[24] S. Rinaldi, S. Muratori, Slow-fast limit-cycles in predator-prey models, Ecol. Model. 61 (1992) 237–388.
[25] S. Schecter, Persistent unstable equilibria and closed orbits of a singularly perturbed equation, J. Differ Equ. 60 (1985) 131–141.
[26] P. Szmolyan, M. Wechselberger, Canards in R3, J. Differ. Equ. 177 (2001) 419–453.
[27] J.T. Tanner, The stability and the intrinsic growth rates of prey and predator populations, Ecology 56 (1975) 855–867.
[28] R.K. Upadhyay, V. Rai, Why chaos is rarely observed in natural populationss, Chaos Solitons Fractals. 8 (12) (1997) 1933–1939.